Desalination and Water Treatment
www.deswater.com
doi: 10.1080/19443994.2013.792133

51 (2013) 6562–6571
October

Taylor & Francis
Taylor & Francis Group

Degradation of methyl orange by electro-Fenton-like process in the presence of chloride ion

Wenyan He[a], Xiaoning Yan[b], Hongzhu Ma[a,*], Jie Yu[a], Jing Wang[a], Xiaoli Huang[a]

[a]*School of Chemistry and Chemical Engineering, Institute of Energy Chemistry, Shaanxi Normal University, Xi'an 710062, China*
Tel. +86 29 81530726; Fax: +86 29 81530727; email: hzmachem@snnu.edu.cn
[b]*Xi'an Hangjie Chemical Technology Co., Ltd, Shaanxi Province 710067, China*

Received 15 February 2012; Accepted 28 January 2013

ABSTRACT

The degradation of azo dye methyl orange (MO) in wastewater by several electrochemical processes, especially the electro-Fenton-like process with chloride ion, was investigated. The effect of some important operating parameters, Fe^{3+} and Cl^- dosage, the initial concentration of MO on the decolorization and COD removal was also investigated. The response surface methodology was selected to optimize the operating conditions, and the results showed that almost 100% color and 78.93% COD removal efficiency were obtained, when $[Fe^{3+}] = 2.14$ mM, $[Cl^-] = 16.36$ mM, $[MO] = 106$ mg L^{-1}, $[Na_2SO_4] = 0.05$ M, pH = 3 at 2.1 A, and approximately 96.93% COD removal was achieved after 90 min of electrolysis and 8 min centrifuged with speed of 500 r min^{-1}. The oxidation kinetics of the process and the reaction order were also studied.

Keywords: Azo dye; Methyl orange; Direct electrochemical process; Electro-Fenton; Response surface methodology; Chloride ion

1. Introduction

Azo-dyes are widely used in our daily life especially in dyeing, printing, textile, cosmetic, and other industries. About over 50% of dyes in common use are azo-dyes because of their chemical stability and versatility, [1] and serious problems were caused to both aquatic life and human beings due to their toxic, carcinogenic, and mutagenic effects [2]. Thus, the treatment of the effluents containing such compounds is necessary.

Various methods for dye removal have been reported [3–6]. However, the complex and steady molecular structure render them resistant to most of technologies, including conventional physical, chemical, and biological treatment. Over the past two decades, as a rapid alternative treatment method, advanced oxidation process (AOP) draw more attention on producing the hydroxyl radicals ($^{\cdot}OH$), a highly powerful oxidizing agent which is capable of oxidizing large variety of organic pollutants [7], yielding dehydrogenated or hydroxylated derivatives, until mineralization [8].

Electro-Fenton oxidation method is an indirect electrochemical AOP with low treatment costs, high efficiency in organic pollutants removal [9], and without requirement for special equipment [10,11], was developed and extensively used for degradation of various organic pollutants including phenolic compounds [12],

*Corresponding author.

1944-3994/1944-3986 © 2013 Balaban Desalination Publications. All rights reserved.

pesticides [13], amines [14], dyes [15] and so on. In the electro-Fenton process, H_2O_2 was generated on the cathode by the reduction of dissolved oxygen in the mild acid aqueous solution [14] (Eq. (1)):

$$O_2 + 2e^- + 2H^+ \rightarrow H_2O_2 \qquad (E^\theta = 0.69\ \text{V/NHE}) \qquad (1)$$

Fe^{2+} can be produced by Fe^{3+} reduction (Eq. (2)) and ($^{\cdot}OH$) generated in situ oxidized the organic matters (Eqs. (3)–(4)):

$$Fe^{3+} + e^- \rightarrow Fe^{2+} \qquad (E^\theta = 0.77\ \text{V/NHE}) \qquad (2)$$

$$Fe^{2+} + H_2O_2 \rightarrow Fe^{3+} + OH^- + {}^{\cdot}OH \qquad (3)$$

$${}^{\cdot}OH + \text{org} \rightarrow CO_2 + H_2O \qquad (4)$$

This process with ($^{\cdot}OH$) production by Fe^{3+} catalyzed H_2O_2 degradation called "electro-Fenton-like" process [13] and catalytic reaction can be propagated via Fe^{2+} regeneration.

Natural water and wastewater contain large amounts of inorganic anions. Generally, the average concentration of chloride ions in groundwater is $3.0 \times 10^{-3}\ \text{mol L}^{-1}$, while in dyes wastewater content is higher. The anion has a significant impact on the electro-Fenton process even if in small amounts [16]. As a crucial factor in the electro-Fenton process, the influence of Cl^- on the degradation of dyes has been carefully investigated. However, much attention has been paid to Cl^-, acted as a hydroxyl radical scavenger which caused decrease of the degradation efficiency in the electro-Fenton process [17], because $ClOH^-$ was formed and reacted with Fe^{2+} during the electro-Fenton process, thus reducing Fe^{2+} then formed ($^{\cdot}OH$). Additionally, in the process of reaction with organic matters, both of the ($^{\cdot}OH$) and Cl^- are involved in oxidation, chlorinated hydrocarbons are observed as products [18]. Besides, the excess of Cl^- can be reacted with Fe^{3+} and formed complex ions with different stabilities.

In this work, we have carefully investigated the influence of Cl^- on the COD removal and decolorization of methyl orange (MO), the oxidation kinetics of the process and the reaction order were also studied. In fact, in this process, Cl^- not only acted as an oxidant but also as a hydroxyl radical scavenger in high concentration. A comparison between the electro-Fenton-like process (EFC) assisted with chloride ions and other electrochemical oxidation processes for MO degradation was carried out. The response surface methodology was selected to optimize the operating conditions, and with the help of the centrifugal force, the COD removal of MO improved significantly.

Table 1
Physicochemical properties of methyl orange

Chemical name	4-dimethylaminoazobenzene-4′-sulfonic acid sodium
Chemical formula	$C_{14}H_{14}N_3NaO_3S$
Chemical structure	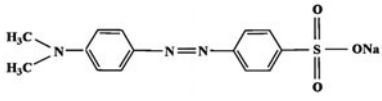
Molecular weight	$327.33\ \text{g mol}^{-1}$
Class	Azo Compounds
Color index	13,025

2. Materials and methods

2.1. Reagents

Azo dye MO (CAS No.: 547-58-0, Table 1 in Supplementary materials), $Fe_2(SO_4)_3{\cdot}7H_2O$, and $FeCl_3{\cdot}6H_2O$, and all chemicals used in the experiment were

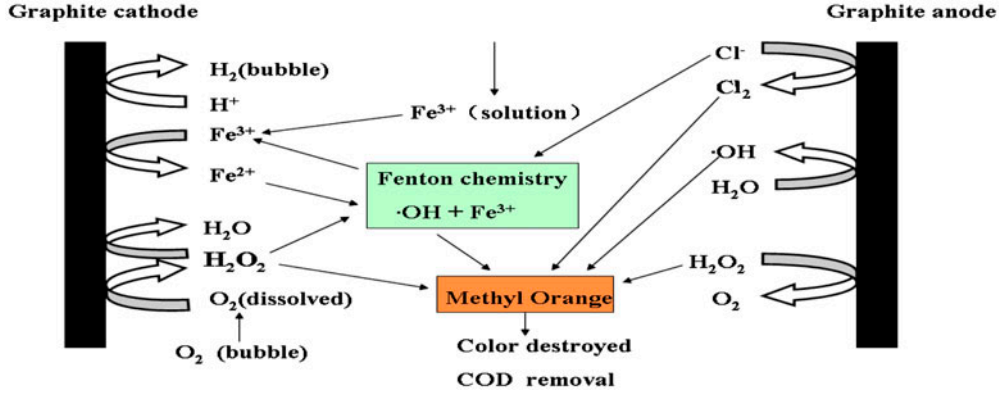

Fig. 1. Sketch of electro-Fenton reaction for MO oxidation.

of analytical grade and used without any further purification. Na_2SO_4 was used as electrolyte, NaOH (0.1 M) or H_2SO_4 (5%) in proper amount was used to get the suitable pH value. Deionized water was used throughout this study.

2.2. Experimental apparatus

An undivided glass electrochemical batch reactor of 1,000 mL with a two-electrode system was used. The anode and cathode were graphite, situated vertically and parallelly to each other with an inner gap of 1 cm (Fig. 1). The superficial surface of working electrode (6.5 cm × 6.5 cm) was 42.25 cm^2. The electric power was supplied by regulated DC power supply (WYK302B2, Xi'An, China), operated at the desired electric current. In addition, an electric mixer was equipped to ensure uniform concentration of the electrolyte solution.

Table 2
Coding of test factors and levels

Factors	Levels		
	−1	0	1
A: Fe^{3+} (mM)	0.5	2.0	3.5
B: Cl^- (mM)	0.6	1.2	1.8
C: MO (mgL^{-1})	50	150	250

2.3. Electro-Fenton-like process

Oxidation of synthetic wastewater containing various concentration of MO by EFC was carried out in 500 mL of 0.05 M Na_2SO_4 solution at pH 3 and 2.1 A. $Fe_2(SO_4)_3{\cdot}7H_2O$ or $FeCl_3{\cdot}6H_2O$ was added at various concentration. NaCl was used to supply the active chlorine at different dosages. In this process, H_2O_2 is produced electrochemically via oxygen reduction on the cathode. For this purpose, continuous saturation of air at atmospheric pressure was ensured by bubbling compressed air sparged near the cathode from the bottom of the cell at about 1 L min^{-1}. The current kept constant during electrolysis and the samples were taken at given time interval from the reactor to be analyzed after filtered or centrifuged.

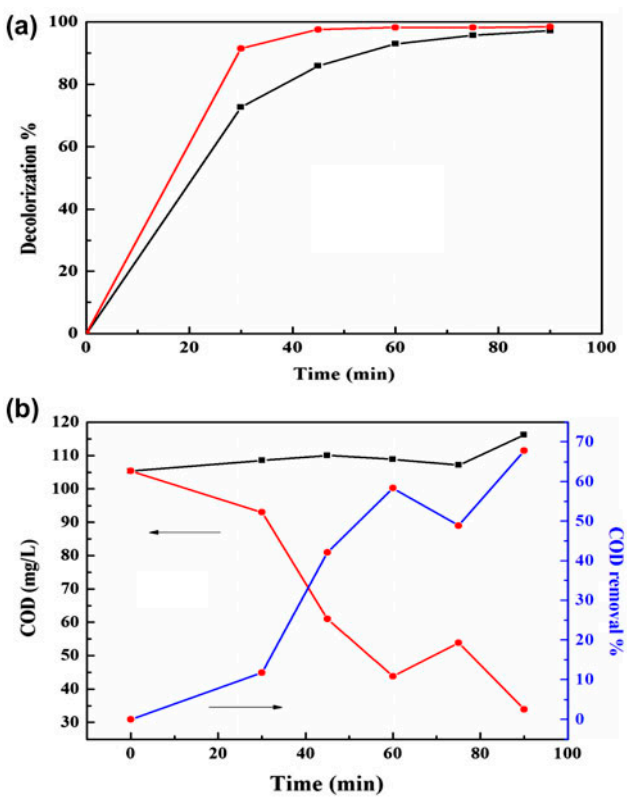

Fig. 2. Comparison of DE (■) and EFC system (●) (a) Decolorization, (b) COD and COD removal ($[MO]_0$ = 100 mg L^{-1}; $[Na_2SO_4]$ = 0.05 M; [NaCl] = 3 mM).

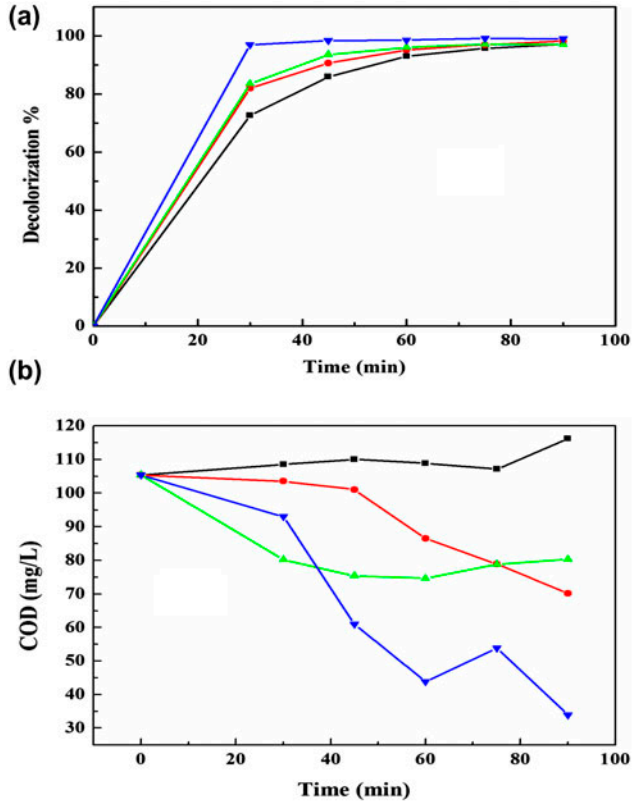

Fig. 3. Comparison of various electrochemical processes (a) decolorization, (b) COD DE(■); EF(●); DEC(▲); EFC(▼). ($[MO]_0$ = 100 mg L^{-1}; $[Na_2SO_4]$ = 0.05 M; [NaCl] = 3 mM).

2.4. Analytical methods

The pH of the solution was measured with a model PHS-3C pH meter. COD removal and decolorization were selected to evaluate the efficiency of the process.

COD values of the solution were measured by COD meter (5B-3(C), Lanzhou, China). The COD removal was calculated by:

$$\text{COD removal}\% = [1 - \text{COD}_t/\text{COD}_0] \times 100\% \quad (5)$$

where COD_0 and COD_t are the COD value ($gO_2\,dm^{-3}$) at reaction time 0 (min) and t (min), respectively.

UV–vis spectra of MO were recorded from 200 to 600 nm using a UV-vis spectrophotometer (UV-7504, China) with a quartz cell (1 cm path length). The maximum absorbance wavelength (λ_{max}) of MO was found at 464 nm. The extent of color removal of the investigated solution can be expressed as:

$$\text{Color removal}\% = (1 - A_t/A_0) \times 100\% \quad (6)$$

where A_0 and A_t are the absorbance of the initial and at reaction time t (min), respectively.

2.5. Statistics method

The experimental results were evaluated with response surface methodology of Design-Expert 7.1, [Fe^{3+}], [Cl^-], and [MO] were selected as the significant factors and the removal of COD was presented by a response function. Table 2 (Supplementary materials) shows three levels of three factors on Box–Behnken Design.

3. Results and discussion

3.1. Comparison of MO degradation by various oxidation processes

3.1.1. Comparison of direct electrolysis and electro-Fenton-like oxidation system

The organic pollutants are thought to be removed from wastewater by direct and indirect processes in the electrochemical system [17]. The decolorization of MO by direct electrolysis oxidation (DE) and the indirect oxidation of EFC with [Cl^-] are shown in Fig. 2 (a). The difference of MO color removal between these two processes is small, indicating that the potential to

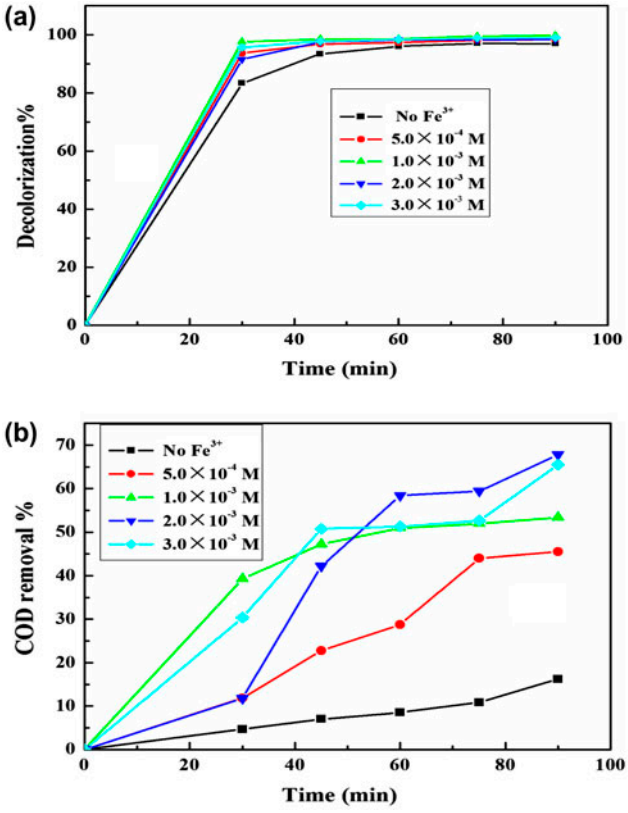

Fig. 4. Effect of [Fe^{3+}] on MO decolorization (a) and COD removal (b) ([Na_2SO_4] = 0.05 M; $[MO]_0$ = 100 mg L^{-1}; [Cl^-] = 6.0 mM).

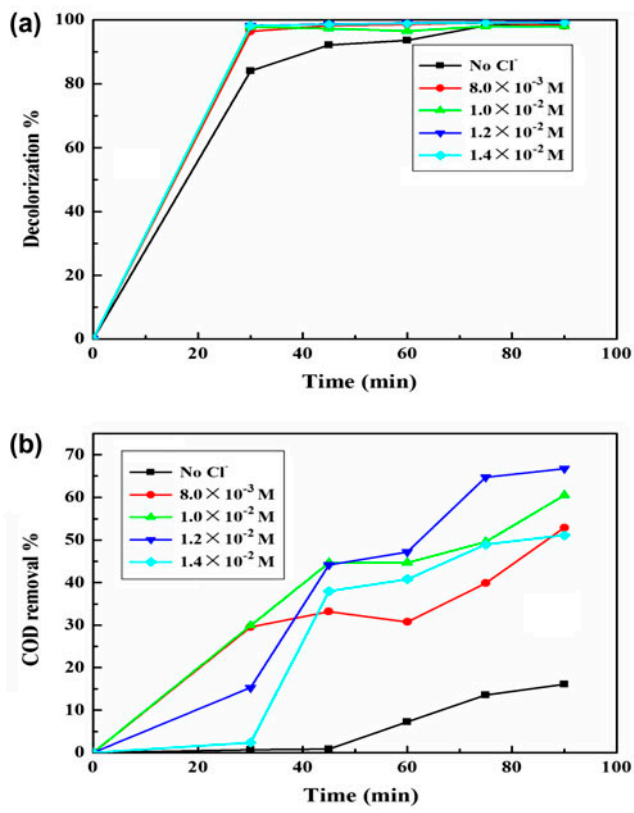

Fig. 5. Effect of [Cl^-] on MO decolorization (a) and COD removal (b) ([Na_2SO_4] = 0.05 M; $[MO]_0$ = 100 mg L^{-1}; [Fe^{3+}] = 2.0 mM).

destroy the –N=N– double bonds in MO molecules, which are attributed to the chroma of the dye, are approximated. However, the COD removal was different evidently in these two electrochemical processes. Fig. 2(b) indicated that the COD removal was not satisfied in the DE process, indicating that the MO degradation was inefficient, this results are also consistent with the reference reported [19]. And 67.79% of COD removal was observed in the EFC, indicating that efficient oxidation has been occurred.

3.1.2. Comparison of different electrochemical processes

In order to study what kind of oxidation species promoted the COD removal efficiency, four various electrochemical systems were investigated: direct electrochemical process with (DEC) or without (DE) Cl^-, EFC with or without (EF) Cl^-, and the results show in Fig. 3. The decolorization follow the order: DE < EF < DEC < EFC in 30 min, indicating that the existence of Cl^- can improve the oxidation properties in the same system. More than 95% of decolorization was achieved after 75 min in EF, DEC, and EFC processes, suggesting that the azo bond –N=N– was almost destroyed completely. And there was no significant difference in Cl^- and ($^{\cdot}OH$) in the decolorization after a longer electrolysis time [20], while the COD removal of MO had effectively increased (Fig. 3(b)).

It can be found that the COD removal of MO was improved in EFC process than that of others, while DE process was inefficient, only 30% COD removal was obtained [21], indicating that the synergistic effect was shown in EFC process. Consequently, EFC process was selected for the degradation of MO in the further study.

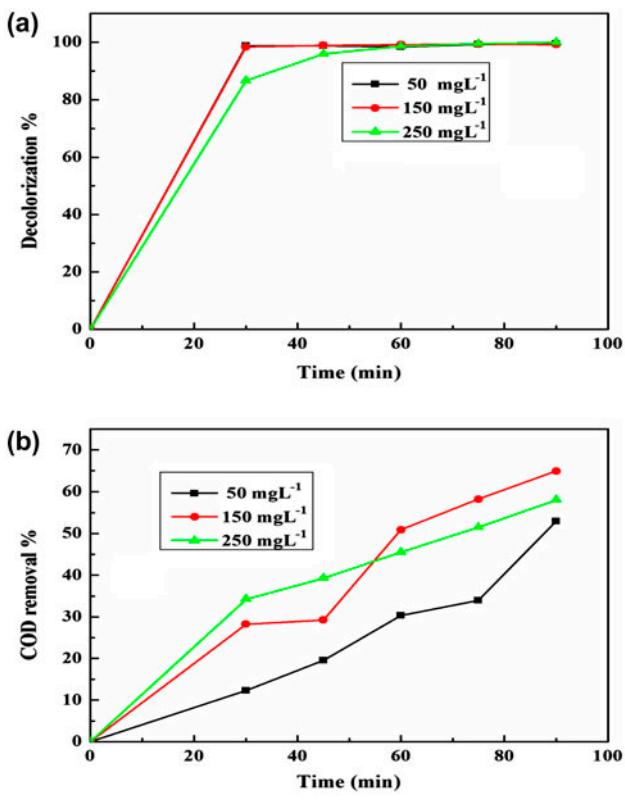

Fig. 6. Effect of $[MO]_0$ on MO decolorization (a) and COD removal (b) ($[Na_2SO_4] = 0.05$ M; $[Cl^-] = 12.0$ mM; $[Fe^{3+}] = 2.0$ mM).

3.2. Optimization of EFC degradation of MO

3.2.1. Effect of ferric ion dosage

The feasibility of using Fe^{3+} rather than Fe^{2+} as catalyst for the decomposition of H_2O_2 to generate ($^{\cdot}OH$) has been extensively investigated [22,23]. The effect of Fe^{3+} dosage on the decolorization and COD removal efficiency of MO was shown in Fig. 4. It was found that the concentration of Fe^{3+} has little effect on the decolorization yet greatly affected COD, and the COD removal increased with the increasing of Fe^{3+}, then decreased when Fe^{3+} was higher than 2.0 mM. This maybe due to that, Fe^{3+} ion at higher concentration will consume the H_2O_2 produced and produce $HO_2\cdot$ species (Eq. (7)) resulting in the decrease of oxidation ability [24].

$$Fe^{3+} + H_2O_2 \rightarrow Fe^{2+} + H^+ + HO_2\cdot \quad (7)$$

Besides, more alkaline chemicals were needed after the electro-Fenton oxidation because of the excessive Fe^{3+}, resulting in the generation of chemical sludge [25]. Consequently, the initial Fe^{3+} concentration was selected as 2.0 mM for further experiments.

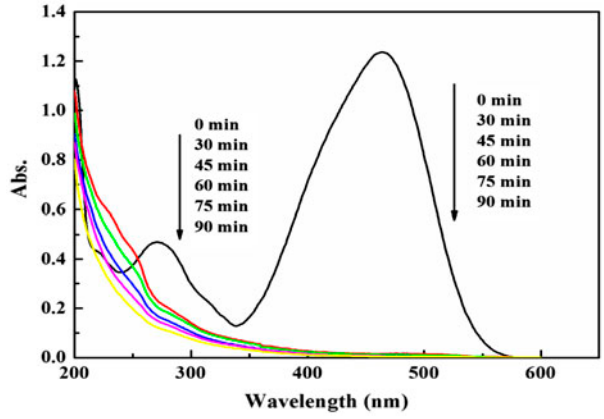

Fig. 7. UV-vis spectra of MO solution ($[Na_2SO_4] = 0.05$ M; $[MO] = 100$ mg L^{-1}; $[Cl^-] = 12.0$ mM; $[Fe^{3+}] = 2.0$ mM).

3.2.2. Effect of chloride ion concentration

100 mg L^{-1} MO was treated by EFC process at pH 3 in the presence of 0.05 M Na_2SO_4 and 2.0 mM Fe^{3+} at 2.1 A with different [Cl^-] (Fig. 5). It can be found that almost 100% decolorization was obtained when Cl^- was introduced. And 12 mM Cl^- enhanced 43.36% COD removal after 45 min, compared to that without Cl^-, while COD removal decreased from 66.73 to 51.13% with Cl^- increasing from 12 to 14 mM after 90 min of electrolysis. Moreover, a large volume of the sludge was formed [26], suggesting that moderate Cl^- can promote the electro-Fenton-like oxidation,

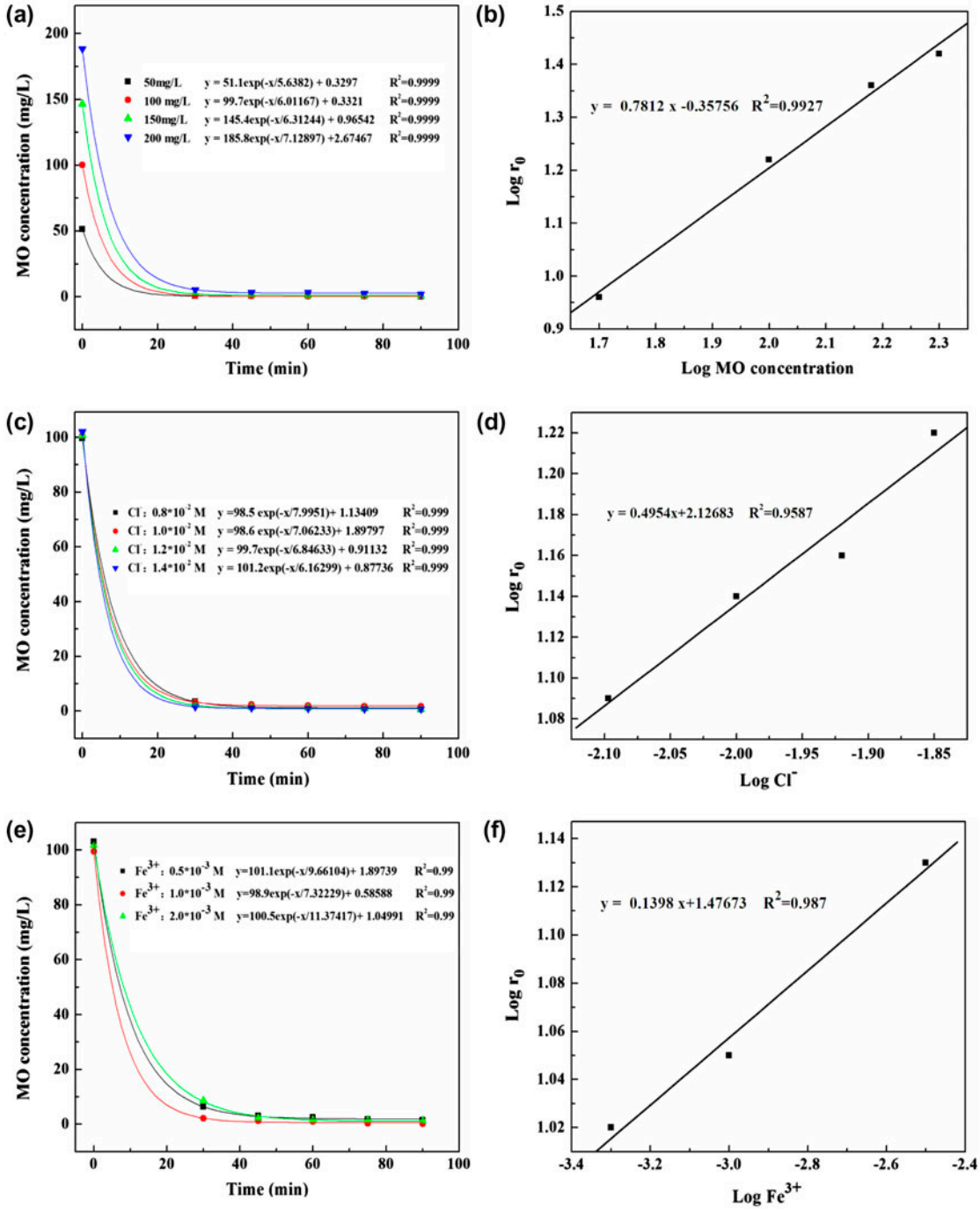

Fig. 8. The relationship of c_0, $-t$ (a, c, e) and the plot of $\log r_0 - \lg c_0$ (b, d, f) (c_0: $[MO]_0$, $[Cl^-]_0$ or $[Fe^{3+}]_0$).

while higher Cl^- would decrease the COD removal efficiency, which is consistent with the references reported [17].

3.2.3. Effect of MO initial concentration

Fig. 6 shows the effect of the initial MO on COD removal and decolorization. When MO increased from 150 to 250 mg L^{-1}, the decolorization decreased from 98.34 to 86.69% within 30 min. When MO increased to a higher level, the amount of OH formed was constant, thus only a small fraction of MO molecules can be degraded, thus led to COD removal and decolorization decreasing, but the extent of MO decolorization reached almost 98% in 60 min, indicating the efficiency of this method on the MO decolorization of destructing the azo N=N bonds [27].

3.3. UV–vis spectra of MO and the kinetics equation

Fig. 7 shows UV–vis spectra of MO under the optimized operational conditions. Two peaks at 464 and 271 nm, attributed to $n \rightarrow \pi^*$ transition of –N=N– group and $\pi \rightarrow \pi^*$ transition of the benzene ring, respectively,

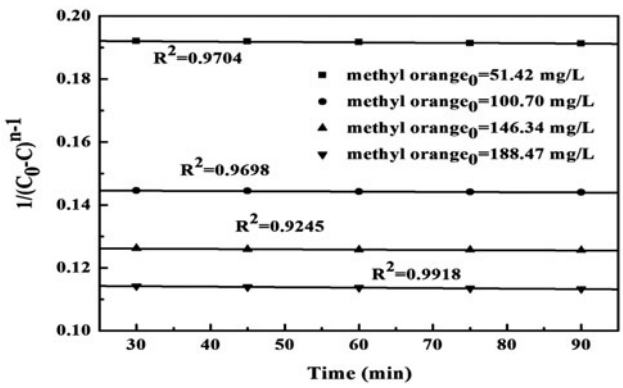

Fig. 9. Plot of $1/(c_0 - c)^{n-1}$ versus time at different $[MO]_0$ (c_0, initial [MO]; c: [MO] at t min in mg/L. $[Cl^-]$ = 12.0 mM; $[Fe^{3+}]$ = 2.0 mM).

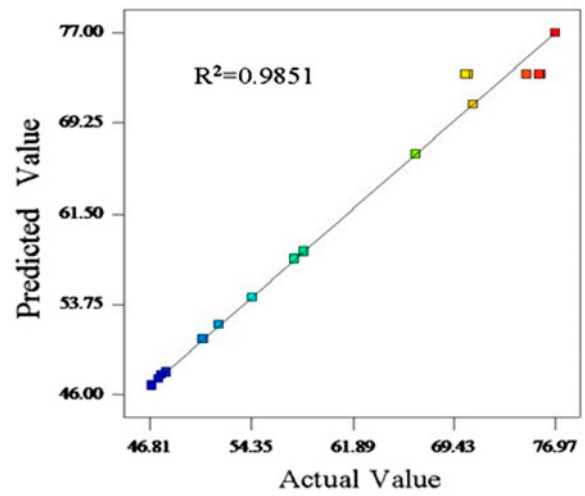

Fig. 10. Parity plot of actual and predicted COD removal for MO wastewater.

Table 3
Results of response surface methodology

No.	Factors			COD removal%		Relative error%
	A	*B*	*C*	Actual	Predicted	
1	−1	−1	0	48.02	47.92	0.21
2	1	−1	0	51.89	51.99	−0.19
3	−1	1	0	46.91	46.81	0.21
4	−1	0	−1	57.56	57.66	−0.17
5	1	0	−1	47.59	47.69	−0.21
6	−1	0	1	54.46	54.36	0.18
7	1	0	1	58.20	58.30	−0.17
8	0	−1	−1	66.65	66.55	0.15
9	0	1	−1	50.76	51.45	−1.34
10	0	−1	1	76.97	76.28	0.90
11	0	1	1	47.40	46.71	1.48
12	0	0	0	70.85	71.54	−0.96
13	0	0	0	70.47	73.43	−4.00
14	0	0	0	75.84	73.43	3.30
15	0	0	0	74.79	73.43	1.85
16	0	0	0	75.81	73.43	3.20
17	0	0	0	70.25	73.43	4.30

Table 4
ANOVA results of the cubic models for COD removal

Source	Sum of squares	Degrees of freedom	Mean square	*F*-value	*P*-value
COD removal (%)					
Model	2135.53	11	194.14	30.07	0.0007
A: Fe^{3+}(mM)	113.00	1	113.00	17.24	0.0089
B: Cl^-(mM)	616.53	1	616.53	95.51	0.0002
C: MO(mgL^{-1})	22.47	1	22.47	3.48	0.1211
AB	11.49	1	11.49	1.78	0.2397
AC	0.62	1	0.62	0.097	0.7684
BC	1.90	1	1.90	0.30	0.6104
A^2	773.46	1	773.46	119.82	0.0001
B^2	324.84	1	324.84	50.32	0.0009
C^2	41.87	1	41.87	6.49	0.0515
A^2B	254.25	1	254.25	39.39	0.0015
A^2C	130.25	1	130.25	20.18	0.0064
Residual	32.28	5	6.46		

R^2 = 0.9851; R^2_{adj} = 0.9524; adequate precision = 14.129.

weakened significantly with the electrolysis proceeded, implying that the relevant structures were destroyed effectively [27].

The oxidation rate of MO in this process can be written as Eq. (8)

$$r = k[Cl^-]^a[Fe^{3+}]^b[MO]^c \quad (8)$$

where r is the reaction rate, k is the rate constant, $[Cl^-]$, $[Fe^{3+}]$, [MO] present the concentration of Cl^-, Fe^{3+}, and MO, respectively.

It can also be rewritten as Eq. (9):

$$\lg r_0 = \lg k_0 + a\lg[Cl^-]_0 + b\lg[Fe^{3+}]_0 + c\lg[MO]_0 \quad (9)$$

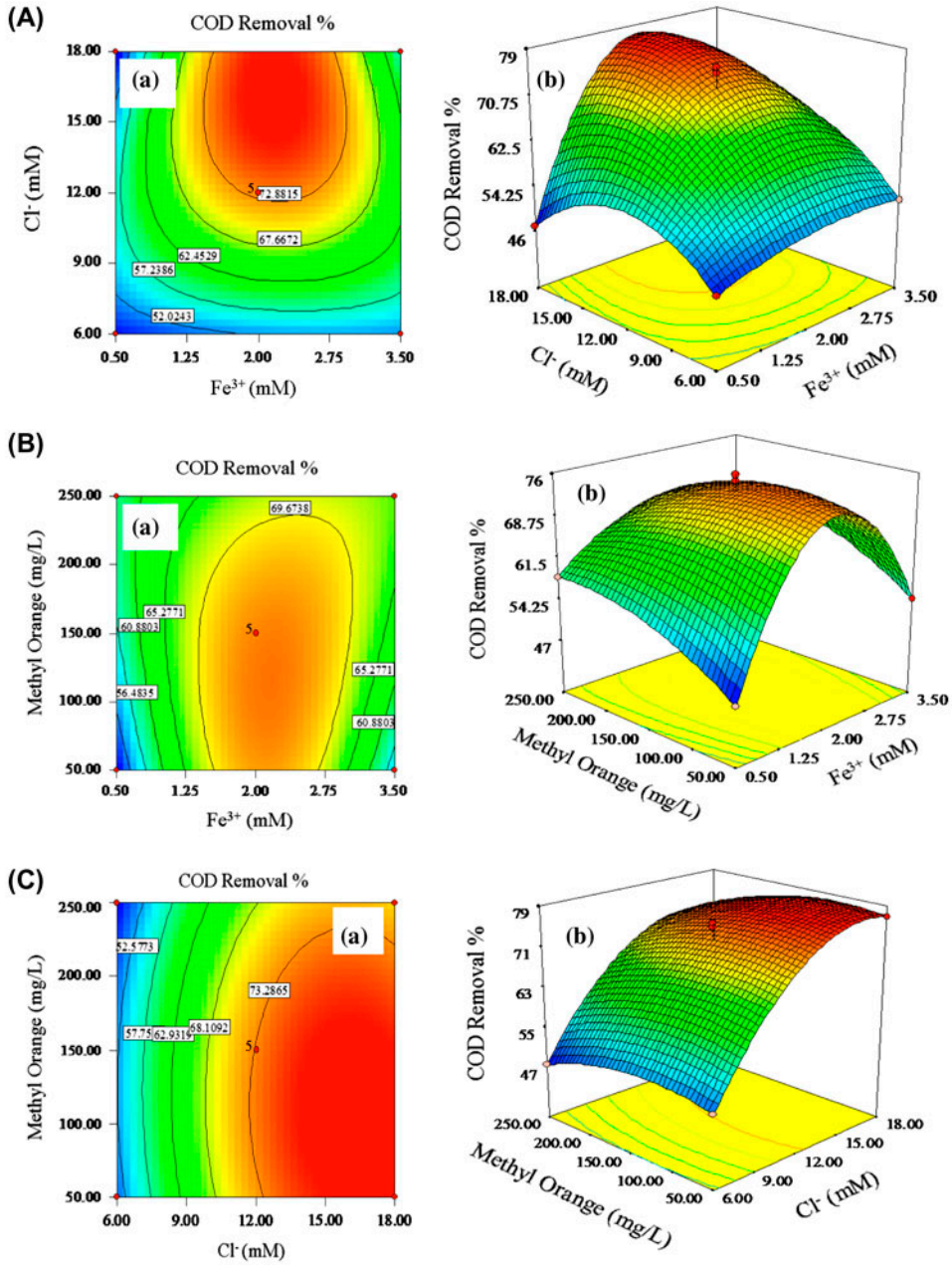

Fig. 11. The interactive effect on COD removal (a) Contour, (b) Response surface plots. (A) $[Cl^-]$ and $[Fe^{3+}]$; (B) [MO] and $[Fe^{3+}]$; (C) [MO] and $[Cl^-]$.

The initial reaction rates were measured from the slope of Fig. 8(a)–(d) at $t = 0$. Therefore, Eqs. ((10)–(12)) can be obtained from Fig. 8(b), (d), and (f):

$$\lg k_0 + 0.1398 \lg[Fe^{3+}]_0 + 0.4954 \lg[Cl^-]_0 = -0.3576 \quad (10)$$

$$\lg k_0 + 0.1398 \lg[Fe^{3+}]_0 + 0.7812 \lg[Cl^-]_0 = 2.1268 \quad (11)$$

$$\lg k_0 + 0.4954 \lg[Fe^{3+}]_0 + 0.7812 \lg[Cl^-]_0 = 1.4767 \quad (12)$$

And $k_0 = 8.4194$ could be obtained. Therefore, the kinetics equation can be listed as:

$$r_0 = 8.4194[Cl^-]_0^{0.4954}[Fe^{3+}]_0^{0.1398}[MO]_0^{0.7812} \quad (13)$$

when $[Cl^-]_0 = 12\,mM$, $[Fe^{3+}]_0 = 2.0\,mM$, $[MO]_0 = 100\,mg/L$, $r_0 = 11933.6\,mg\,L^{-1}\,min^{-1}$, means that this process has a very fast oxidation rate at the very beginning. The obvious reaction order 1.4164 is also confirmed by Fig. 9.

3.4. Optimization of experimental conditions with response surface methodology

The experimental design and the results are shown in Table 3 (Supplementary materials). It can be found that the relative error between the predicted value and the experimental value was less than 5%. In addition, the actual experimental data distribution was consistent with the predicted data distribution (Fig. 10), indicating that the model applied to this system is feasible.

Analysis of variance (ANOVA) tests for COD removal were conducted to determine the suitability of the response function and the significance of variables effects on the response function (Table 4 in Supplementary materials). Model *F*-value of 30.07 implies the model which is significant for COD removal. The effect of experimental factors on response at optimized conditions showed in Fig. 11. It can be found that, Cl^- has the most important effect on the COD removal, while MO has little significant influence.

Based on the above discussions, the optimal operation conditions for fast and efficient oxidation of MO by EFC process were: [MO] $106\,mg\,L^{-1}$, $[Cl^-]$ 16.36 mM, at pH 3, $[Na_2SO_4]$ 0.05 M, and $[Fe^{3+}]$ 2.14 mM at 2.1 A, the highest COD removal can reach 78.93%.

About 96.93% COD removal was obtained when centrifuged for 8 min after 90 min of electrolysis in EFC process and an increase of 20.42% COD was observed. It shows that the electrolysis process was improved and promoted by the centrifugal force, so that the COD removal rate increased significantly.

4. Conclusion

In this work, EFC with the synergistic effect of Cl^- was selected as an efficient method for MO degradation. The optimum operating condition was optimized by the response surface methodology; more than 78.93% of COD removal and almost 100% decolorization were achieved within 90 min. Moreover, low Cl^- dosage can promote the degradation of MO but further increasing of Cl^- has negative effect on COD removal of MO. It was also found that the COD removal was significant with centrifugation, the reason of this phenomenon would be further studied.

References

[1] M. Neamtu, I. Siminiceanu, A. Yadiler, A. Kettrup, Kinetic of decolorization and mineralization of reactive azo dyes in aqueous solution by the UV/H_2O_2 oxidation, Dyes Pigm. 53 (2002) 93–99.
[2] K.C. Chen, J.Y. Wu, C.C. Huang, Y.M. Liang, Decolorization of azo dye using PVA-immobilized microorganisms, J. Biotechnol. 101 (2003) 241–250.
[3] J. Wu, F. Liu, H. Zhang, J.H. Zhang, L. Li, Decolorization of CI Reactive Black eight by electrochemical process with/without ultrasonic irradiation, Desalin. Water Treat. 44 (2012) 36–43.
[4] M. Sarioglu, T. Bisgin, Decolorization of basic red 46 and methylene blue by anaerobic sludge: Biotic and abiotic processes, Desalin. Water Treat. 23 (2010) 61–65.
[5] A. Baraka, Adsorptive removal of tartrazine and methylene blue from wastewater using melamine-formaldehyde-tartaric acid resin (and a discussion about pseudo second order model), Desalin. Water Treat. 44 (2012) 128–141.
[6] K. Umar, A.A. Dar, M.M. Haque, N.A. Mir, M. Muneer, Photocatalysed decolourization of two textile dye derivatives, martius yellow and acid Blue 129, in UV-irradiated aqueous suspensions of Titania, Desalin. Water Treat. 46 (2012) 205–214.
[7] E. Brillas, M.A. Banos, J.A. Garrido, Mineralization of herbicide 3,6-dichloro-2- methoxybenzoic acid in aqueous medium by anodic oxidation, electro-Fenton and photoelectro-Fenton, Electrochim. Acta 48 (2003) 1697–1705.
[8] H.S. El-Desoky, M.M. Ghoneim, R. El-Sheikh, N.M. Zidan, Oxidation of Levafix CA reactive azo-dyes in industrial wastewater of texitile dyeing by electro-generated Fenton's reagent, J. Hazard. Mater. 175 (2010) 858–865.
[9] M.M. Gao, G.H. Zhang, X.H. Wang, F.L. Yang, The bromamine acid removal from aqueous solution using electro-Fenton and Fenton systems, Desalin. Water Treat. 47 (2012) 157–162.

[10] S. Hammami, N. Oturan, N. Bellakhal, M. Dachraoui, M.A. Oturan, Oxidative degradation of direct orange 61 by electro-Fenton process using a carbon felt electrode: application of the experiment design methodology, J. Electroanal. Chem. 610 (2007) 75–84.
[11] C.A. Martínez-Huitle, E. Brillas, Decontamination of wastewaters containing synthetic organic dyes by electrochemical methods: A general review, Appl. Catal. B Environ. 87 (2009) 105–145.
[12] M.A. Oturan, J. Peiroten, P. Chartrin, A.J. Acher, Complete destruction of p-nitrophenol in aqueous medium by electro-Fenton method, J. R. Environ. Sci. Technol. 34 (2000) 3474–3479.
[13] N. Oturan, M.H. Zhou, M.A. Oturan, Metomyl degradation by electro-Fenton and electro-Fenton-like processes: A kinetics study of the effect of the nature and concentration of some transition metal ions as catalyst, J. Phys. Chem. A 114 (2010) 10605–10611.
[14] W.P. Ting, M.C. Lu, Y.H. Huang, Kinetics of 2,6-dimethylaniline degradation by electro-Fenton process, J. Hazard. Mater. 161 (2009) 1484–1490.
[15] M. Panizza, G. Cerisola, Electro-Fenton degradation of synthetic dyes, Water Res. 43 (2009) 339–344.
[16] X.Y. Yu, Critical evaluation of rate constants and equilibrium constants of hydrogen peroxide photolysis in acidic aqueous solutions containing chlorine ions, J. Phys. Chem. Ref. Data 33 (2004) 747–764.
[17] B.K. Körbahti, A. Tanyolac, Continuous electrochemical treatment of simulated industrial textile wastewater from industrial components in a tubular reactor, J. Hazard. Mater. 170 (2009) 771–778.
[18] J. KiWi, A. Lopez, V. Nadtochenko, Mechanism and kinetics of the OH-radical intervention during Fenton oxidation in the presence of a significant amount of radical scavenger (Cl^-), Environ. Sci. Technol. 34 (2000) 2162–2168.
[19] A. özcan, M.A. Oturan, N. Oturan, Y. Sahin, N. Oturan, Removal of acid orange seven from water by electrochemically generated Fenton's reagent, J. Hazard. Mater 163 (2009) 1213–1220.
[20] A. Wang, J. Qu, J. Ru, H. Liu, J. Ge, Minerlization of an azo dye red 14 by electro-Fenton's reagent using an activated carbon fider cathode, Dyes Pigm. 65 (2005) 227–233.
[21] C.T. Wang, J.L. Hu, W.L. Chou, Y.M. Kuo, Removal of color from real dyeing wastewater by electro-Fenton technology using a three-dimensional graphite cathode, J. Hazard. Mater. 152 (2008) 601–606.
[22] I. Sirés, J.A. Garrido, R.M. Rodríguez, E. Brillas, N. Oturan, M.A. Oturan, Catalytic behavior of the Fe^{3+}/Fe^{2+} system in the electro-Fenton degradation of the antimicrobial chlorophene, Appl. Catal. B 72 (2007) 382–394.
[23] E. Brillas, B. Boye, I. Sirés, J.A. Garrido, R.M. Rodríguez, C. Arias, P.L. Cabot, C. Comninellis, Electrochemical destruction of chlorophenoxy herbicides by anodic oxidation and electro-Fenton using a boron-doped diamond electrode, Electrochim. Acta 49 (2004) 4487–4496.
[24] W. Luo, M.E. Abbas, L.H. Zhu, K.J. Deng, H.Q. Tang, Rapid quantitative determination of hydrogen peroxide by oxidation decolorization of methyl orange using a Fenton reaction system, Anal. Chim. Acta 629 (2008) 1–5.
[25] Y.Y. Chu, Y. Qian, W.J. Wang, X.L. Deng, A dual-cathode electro-Fenton oxidation coupled with anodic oxidation system used for 4-nitrophenol degradation, J. Hazard. Mater. 199–200 (2012) 179–185.
[26] S. Mahesh, B. Prasad, I.D. Mall, I.M. Mishra, Electrochemical degradation of pulp and paper mill wastewater. Part 1. COD and color removal, Ind. Eng. Chem. Res. 45 (2006) 2830–2839.
[27] X.J. Ma, M.H. Zhou, A comparative study of azo dye decolorization by electro-Fenton in two common electrolytes, J. Chem. Technol. Biotechnol. 84 (2009) 1544–1549.